

# **MODELING OF MICRODISCHARGES FOR USE AS MICROTHRUSTERS**

**Ramesh A. Arakoni<sup>a)</sup> , J. J. Ewing<sup>b)</sup> and Mark J. Kushner<sup>c)</sup>**

**a) Dept. Aerospace Engineering  
University of Illinois**

**b) Ewing Technology Associates**

**c) Dept. Electrical Engineering  
Iowa State University**

**mjk@iastate.edu, arakoni@uiuc.edu, jjewingta@comcast.net  
<http://uigelz.ece.iastate.edu>**

**52<sup>nd</sup> AVS International Symposium,  
November 2, 2005.**

**\* Work supported by Ewing Technology Associates, NSF, and AFOSR.**

# AGENDA

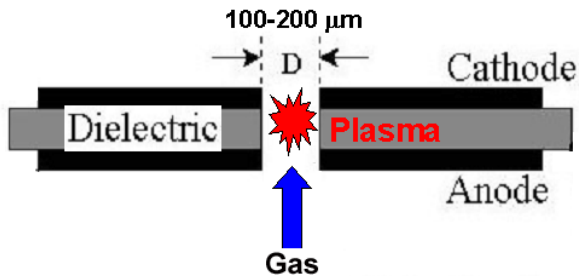
---

- **Introduction to microdischarge (MD) devices**
- **Description of model**
- **Reactor geometry and parameters**
- **Plasma characteristics**
- **Effect of geometry, and power**
- **Incremental thrust, and effect of power**
- **Concluding Remarks**

# MICRODISCHARGE PLASMA SOURCES

---

- Microdischarges are plasma devices which leverage pd scaling to operate dc atmospheric glows 10s –100s  $\mu\text{m}$  in size.
- Few 100s V, a few mA
- Although similar to PDP cells, MDs are usually dc devices which largely rely on nonequilibrium beam components of the EED.
- Electrostatic nonequilibrium results from their small size. Debye lengths and cathode falls are commensurate with size of devices.



$$L_{cathode\,Fall} = \left(2V_c \epsilon_0 / (qn_I)\right)^{1/2} \approx 10 - 20 \mu\text{m}$$

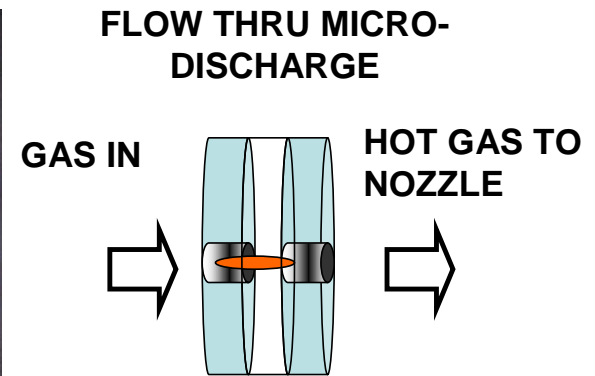
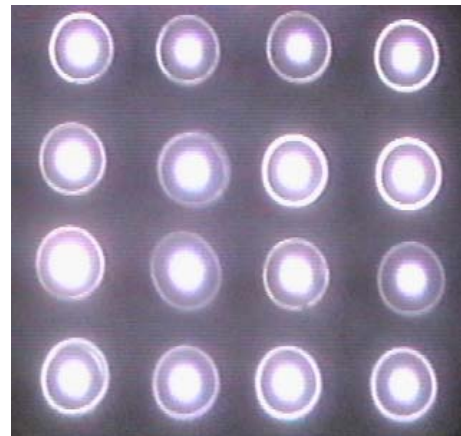
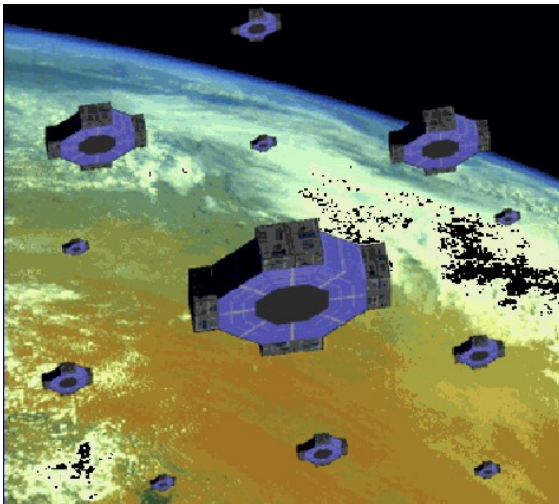
$$\lambda_D \approx 750 \left( \frac{T_{eV}}{n_e (cm^{-3})} \right)^{1/2} cm \approx 10 \mu\text{m},$$

- Ref: Kurt Becker, GEC 2003

# APPLICATIONS OF MICRODISCHARGES

---

- **MEMS fabrication techniques enable innovative structures for displays and detectors.**
- **MDs can be used as microthrusters in small spacecraft for precise control which are requisites for array of satellites.**



**Ewing Technology  
Associates**

Ref: <http://www.design.caltech.edu/micropropulsion>

# DESCRIPTION OF MODEL

---

- **To investigate microdischarge sources, nonPDPSIM, a 2-dimensional plasma code was developed with added capabilities for pulsed operation.**
  - **Finite volume method in rectilinear or cylindrical unstructured meshes.**
  - **Implicit drift-diffusion-advection for charged species**
  - **Navier-Stokes for neutral species**
  - **Poisson's equation (volume, surface charge, material conduction)**
  - **Secondary electrons by impact, thermionics, photo-emission**
  - **Electron energy equation coupled with Boltzmann solution**
  - **Monte Carlo simulation for beam electrons.**
  - **Circuit, radiation transport and photoionization, surface chemistry models.**

# DESCRIPTION OF MODEL: CHARGED PARTICLE, SOURCES

---

- **Continuity (sources from electron and heavy particle collisions, surface chemistry, photo-ionization, secondary emission), fluxes by modified Sharfetter-Gummel with advective flow field.**

$$\frac{\partial N_i}{\partial t} = -\vec{\nabla} \cdot \vec{\phi} + S_i$$

- **Poisson's Equation for Electric Potential:**  $-\nabla \cdot \epsilon \nabla \Phi = \rho_V + \rho_S$
- **Photoionization, electric field and secondary emission:**

$$S_{Pi}(\vec{r}) = \int \frac{N_i(\vec{r}) \sigma_{ij} N_j(\vec{r}') \exp\left(\frac{-|\vec{r}' - \vec{r}|}{\lambda}\right) d^3\vec{r}'}{4\pi |\vec{r}' - \vec{r}|^2}$$

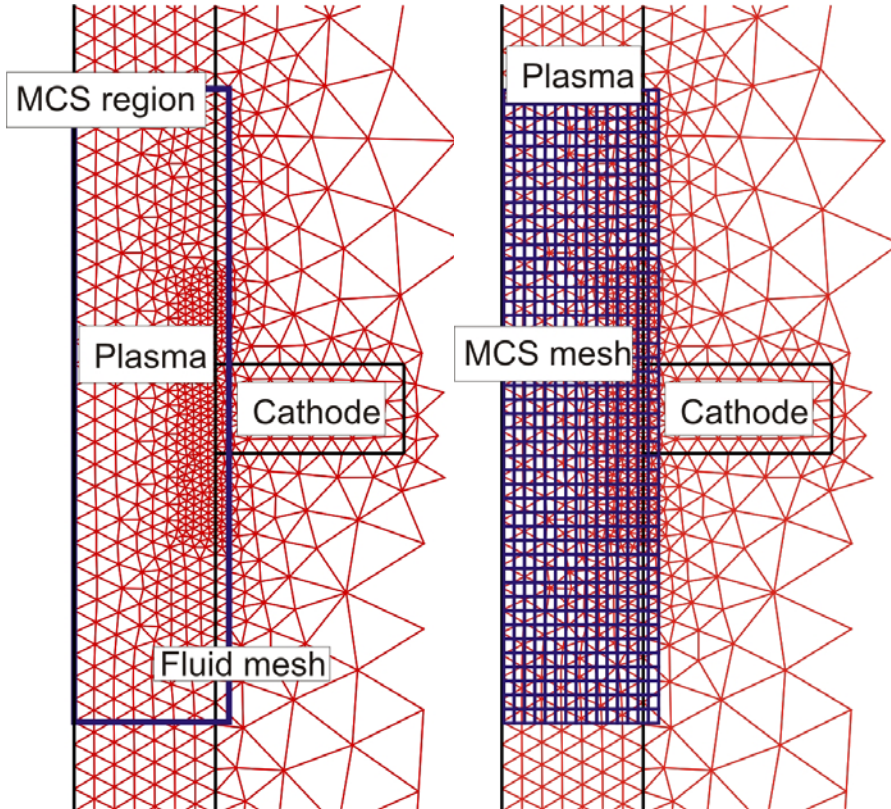
$$S_{Si} = -\nabla \cdot \mathbf{j}, \quad j_E = AT^2 \exp\left(\frac{-\left(\Phi_W - (q^3 E / \epsilon_0)^{1/2}\right)}{kT_S}\right), \quad j_S = \sum_j \gamma_{ij} \phi_j$$

# ELECTRON ENERGY, TRANSPORT COEFFICIENTS

---

- **Bulk electrons:** Electron energy equation with coefficients obtained from Boltzmann's equation solution for EED.

$$\frac{\partial(n_e \varepsilon)}{\partial t} = \vec{j} \cdot \vec{E} + \sigma E_{EM}^2 - n_e \sum_i N_i \kappa_i - \nabla \cdot \left( \frac{5}{2} \varepsilon \phi - \lambda \nabla T_e \right), \quad \vec{j} = q \vec{\phi}_e$$



- **Beam Electrons: Monte Carlo Simulation**
- **Cartesian MCS mesh superimposed on unstructured fluid mesh. Construct Greens functions for interpolation between meshes.**

# DESCRIPTION OF MODEL: NEUTRAL PARTICLE TRANSPORT

---

- Fluid averaged values of mass density, mass momentum and thermal energy density obtained using unsteady, compressible algorithms.

$$\frac{\partial \rho}{\partial t} = -\nabla \cdot (\rho \vec{v}) + (\text{inlets, pumps})$$

$$\frac{\partial(\rho \vec{v})}{\partial t} = \nabla \left( \sum_i N_i k T_i \right) - \nabla \cdot (\rho \vec{v} \vec{v}) - \vec{\nabla} \cdot \vec{\tau} + \sum_i \left( q_i N_i \vec{E}_i - S_i m_i \mu_i q_i \vec{E} \right)$$

$$\frac{\partial(\rho c_p T)}{\partial t} = -\nabla \cdot (-\kappa \nabla T + \rho \vec{v} c_p T) + P_i \nabla \cdot \vec{v}_f - \sum_i R_i \Delta H_i + \sum_i \vec{j}_i \cdot \vec{E}$$

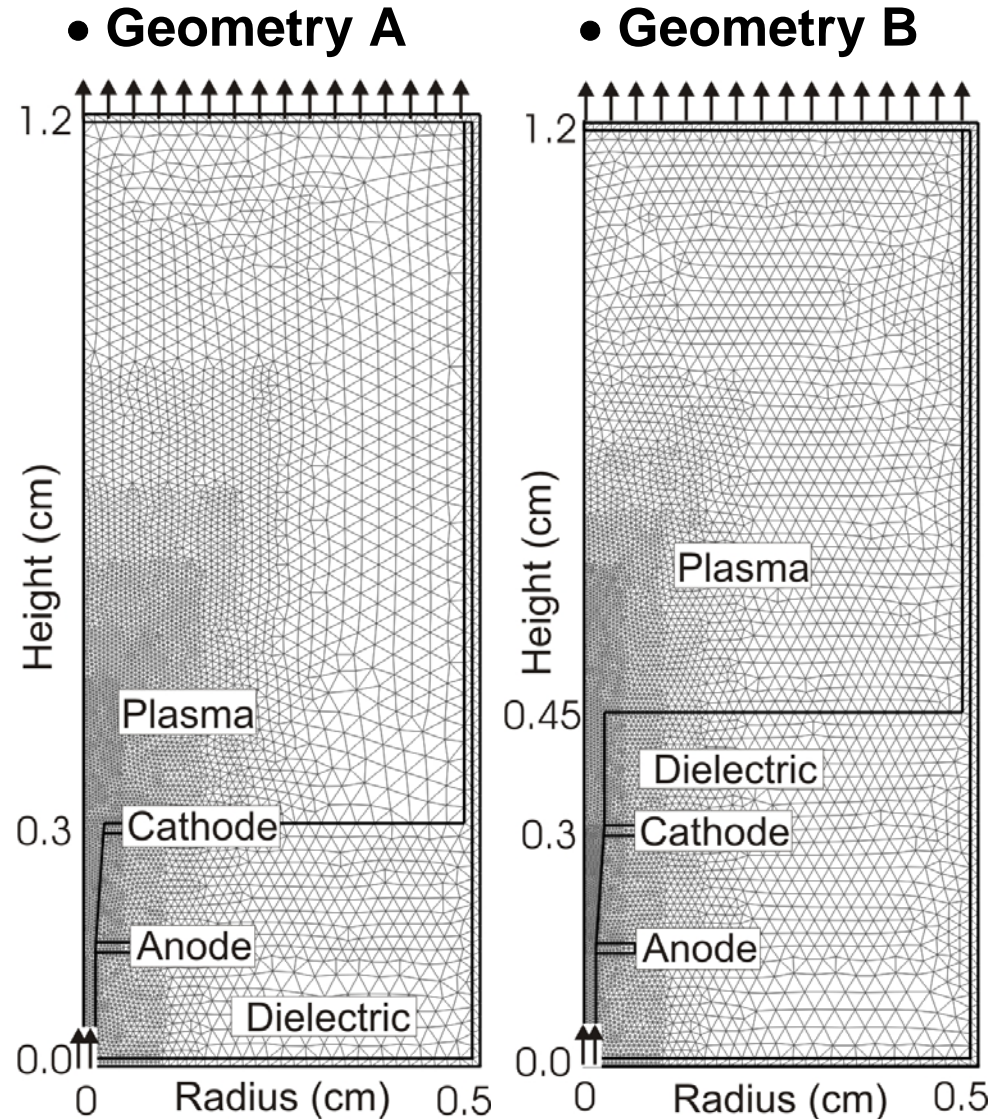
- Individual species are addressed with superimposed diffusive transport.

$$N_i(t + \Delta t) = N_i(t) - \nabla \cdot \left( \vec{v}_f - D_i N_T \nabla \left( \frac{N_i(t + \Delta t)}{N_T} \right) \right) + S_V + S_S$$



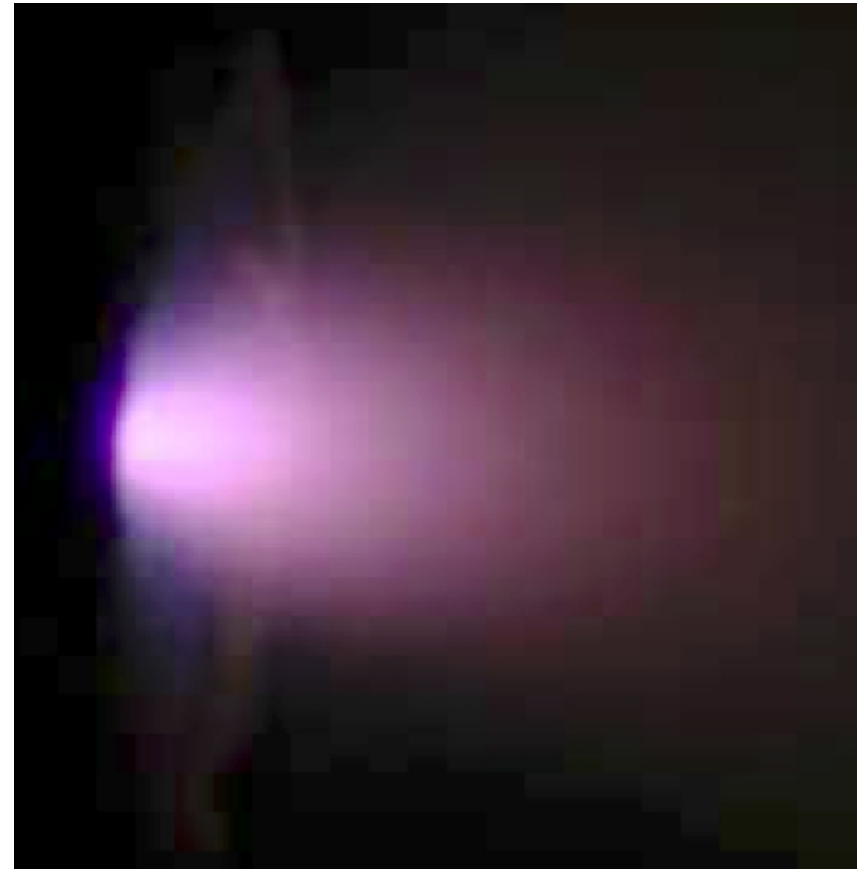
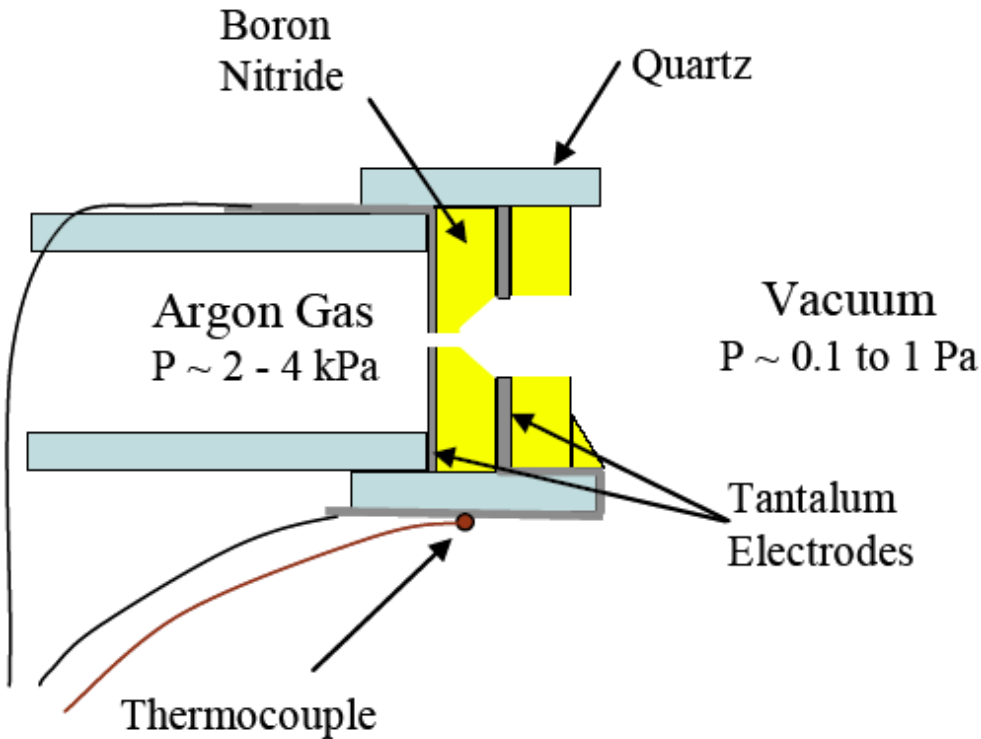
# GEOMETRY AND MESH

- Plasma dia: 150  $\mu\text{m}$  at inlet, 250  $\mu\text{m}$  at cathode.
- Electrodes 130  $\mu\text{m}$  thick.
- Dielectric gap 1.5 mm.
- Geometry B: 1.5 mm dielectric above the cathode.
- Fine meshing near electrodes, less refined near exit.
- Anode grounded; cathode bias varied based on power deposition (0.25 - 1.0 W).
- 10 sccm Ar, 30 Torr at inlet, 10 Torr at exit.



# EXPERIMENT: GEOMETRY

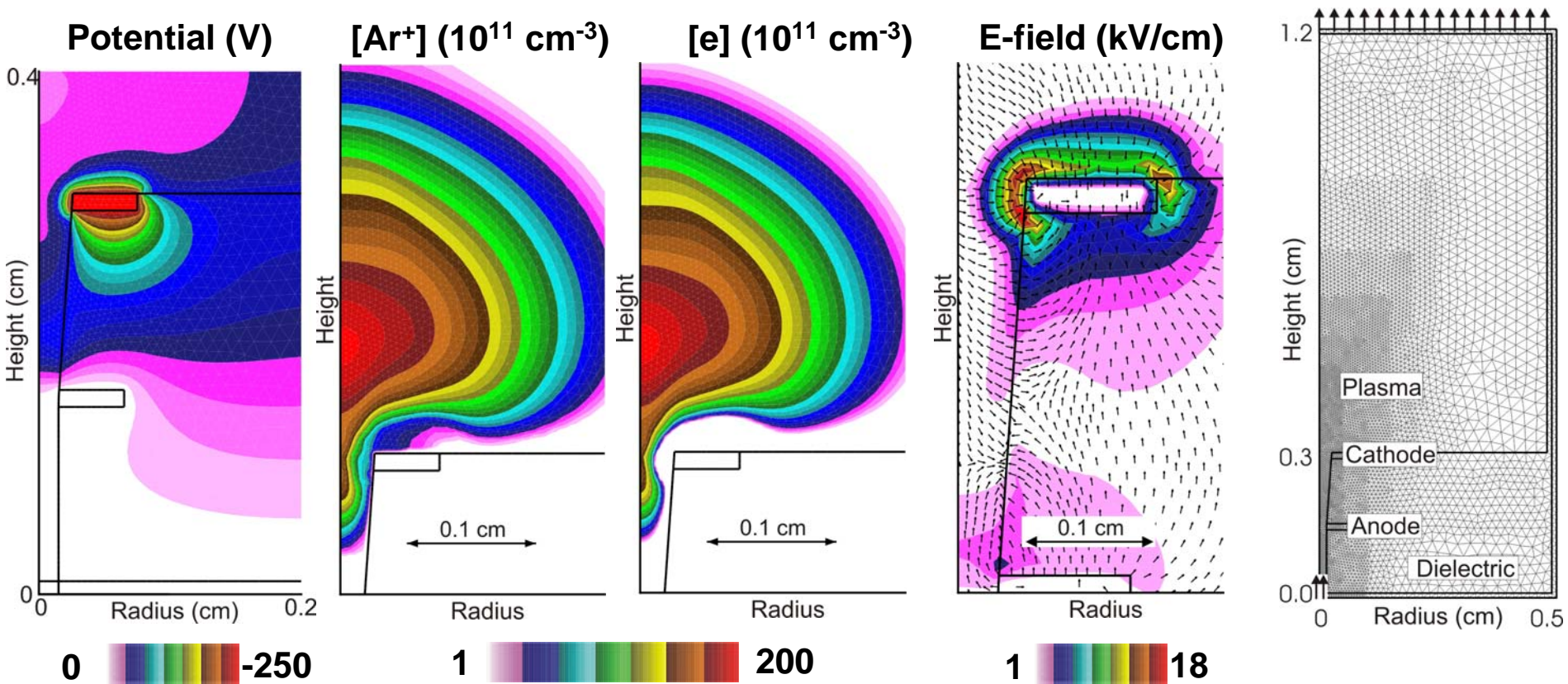
---



- Modeled geometry similar to experimental setup.
- Plume characterized by densities of excited states.

• Ref: John Slough, J.J. Ewing, AIAA 2005-4074

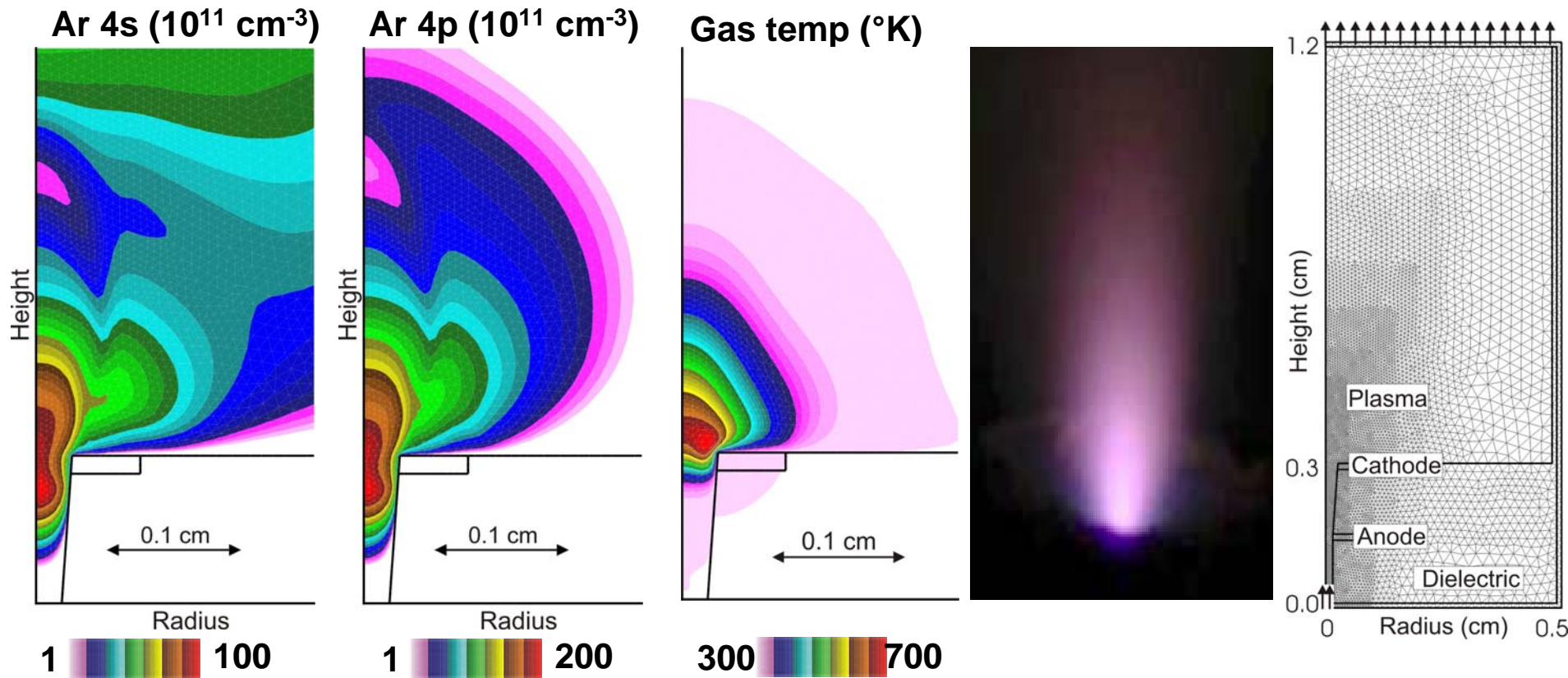
# CHARGED SPECIES: GEOMETRY A



- Power deposition occurs in the cathode fall by collisions with hot electrons.
- Very high electric fields near cathode.

• 10 sccm Ar, 0.5 W

# NEUTRAL FLUID PROPERTIES: GEOMETRY A



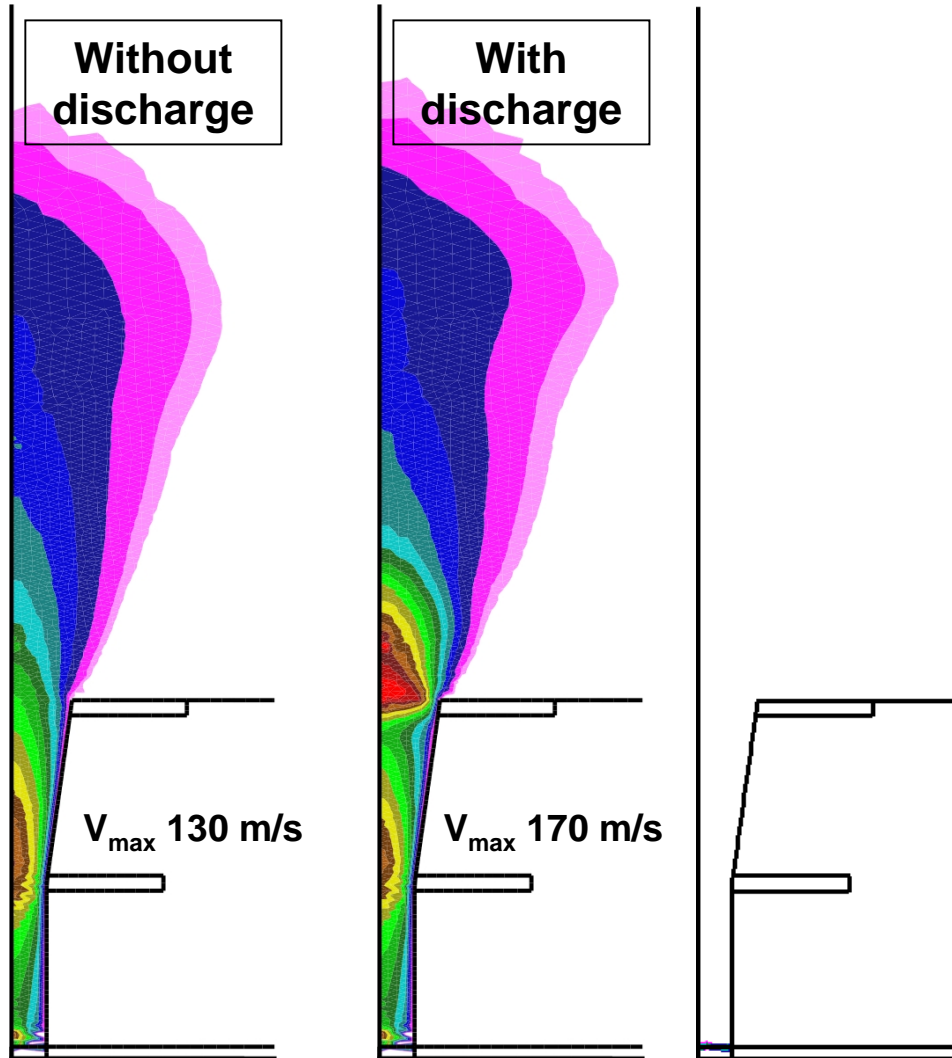
- **Plume extends downstream, can be used for diagnosis.**
- **Gas heating and consequent expansion is a source of thrust.**

- **10 sccm Ar, 30 – 10 Torr**
- **0.5 W.**

• Ref: John Slough, J.J. Ewing, AIAA 2005-4074

Iowa State University  
Optical and Discharge Physics

# VELOCITY INCREASE WITH DISCHARGE



0  160  
Axial velocity (m/s)

AVS2005\_RAA\_12

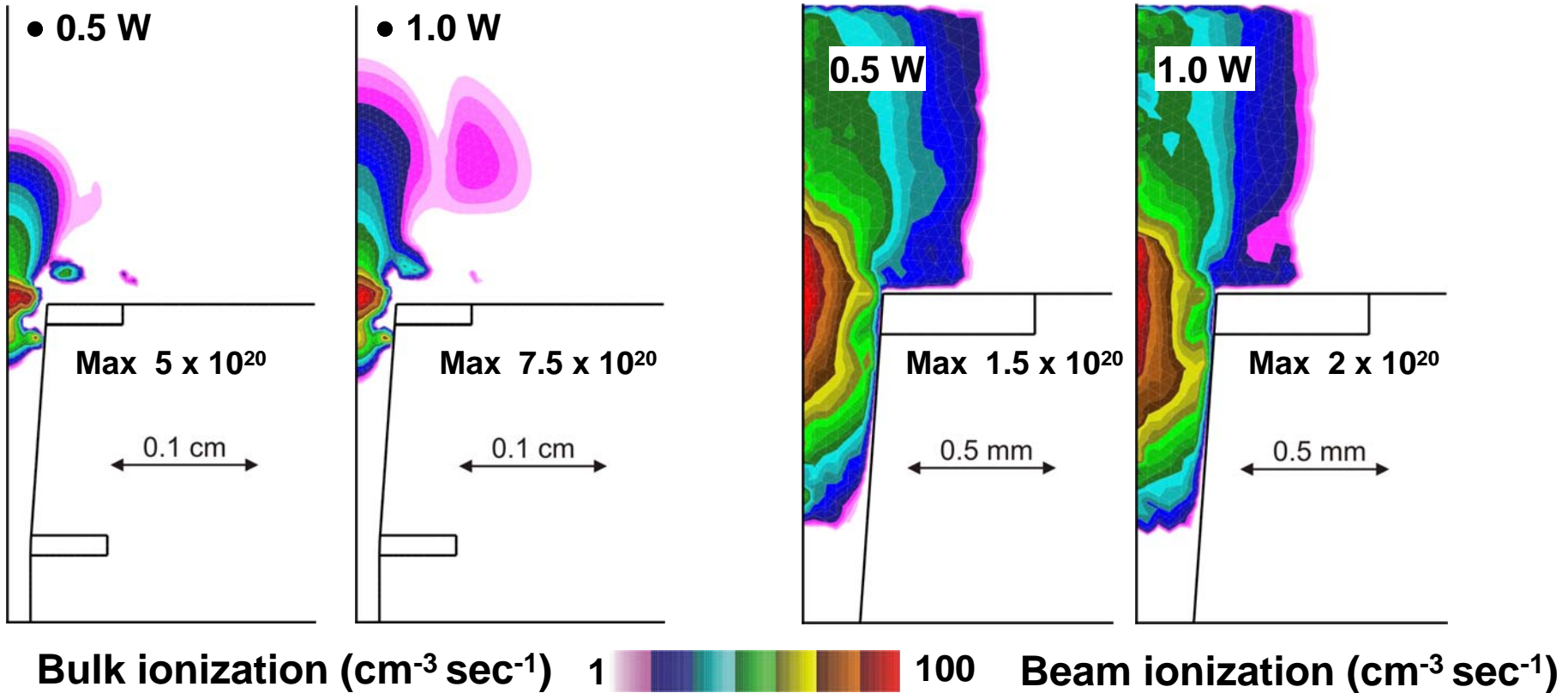
Animation  
0 – 0.55 ms

- Gas heating and subsequent expansion causes increase in velocity.
- Steady state after one or two bursts of flow.
- At high plasma density, momentum transfer between charged species and neutrals is also important.

- 10 sccm Ar, 30 Torr at inlet, 10 Torr at exit.
- 0.5 Watts.
- Power turned on at 0.5 ms.

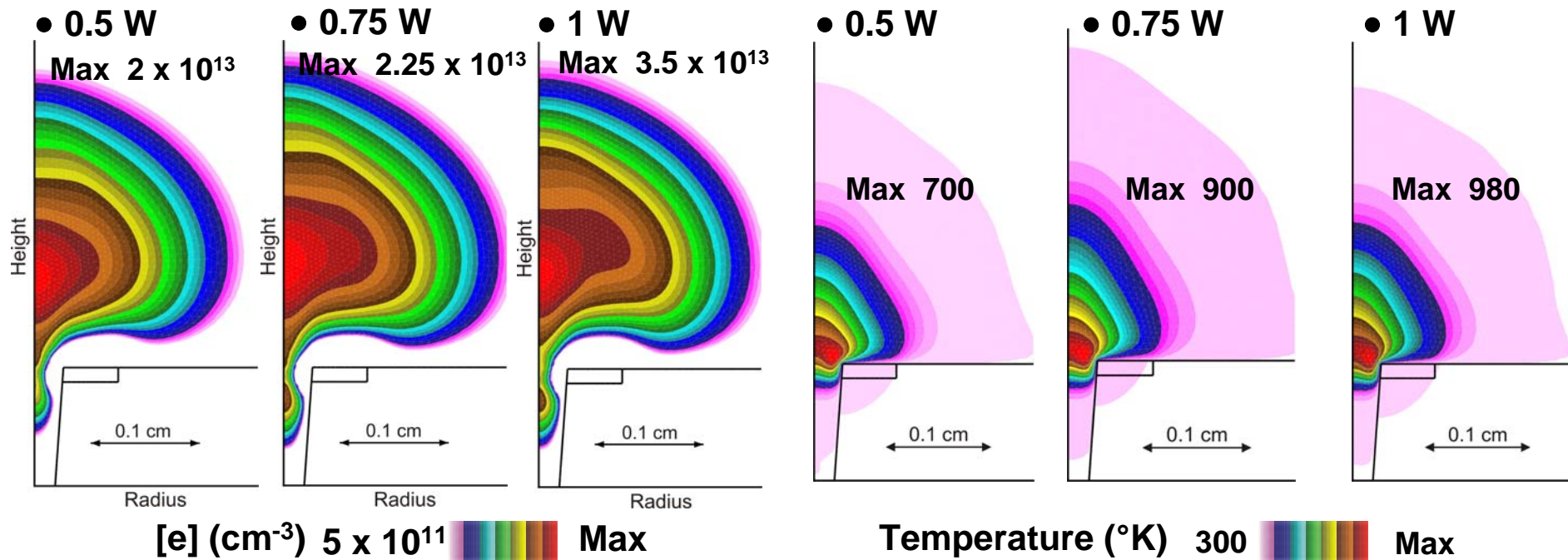
Iowa State University  
Optical and Discharge Physics

# POWER DEPOSITION: IONIZATION SOURCES



- Ionization rates increase with power.
- Beam electrons are equally as important as bulk electrons.
- 10 sccm Ar, 30 Torr at inlet, 10 Torr at exit.

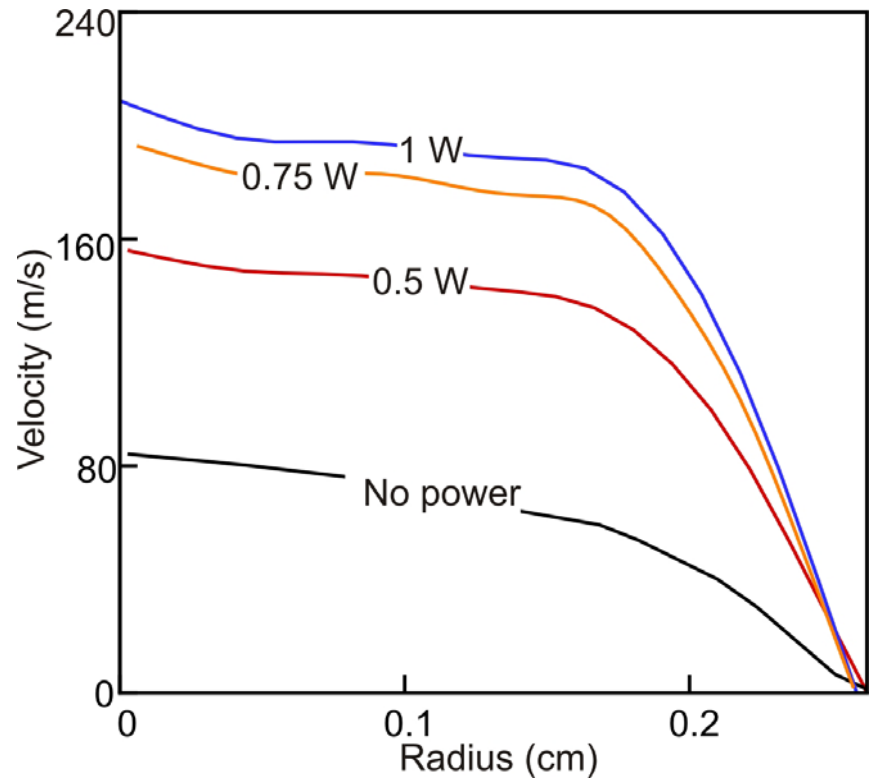
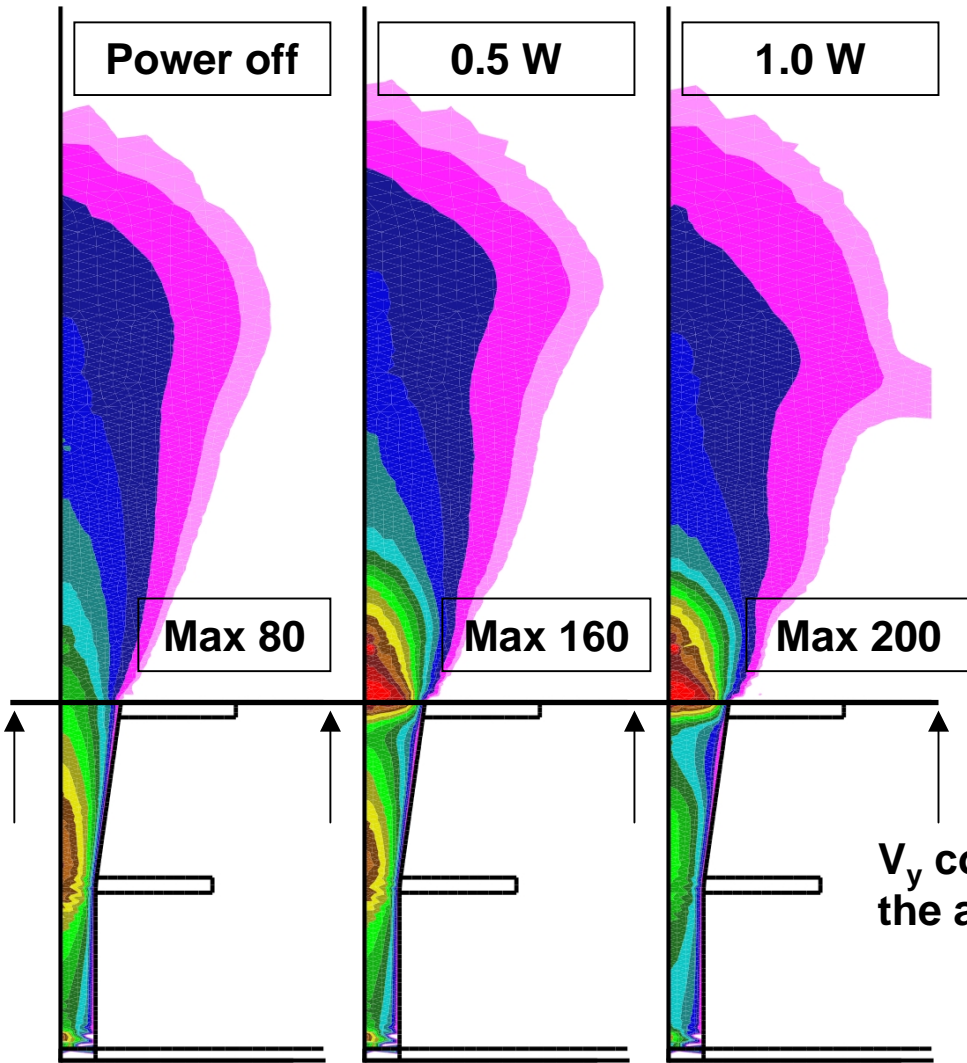
# POWER DEPOSITION: PLASMA PROPERTIES



- Hotter gases lead to higher  $\Delta V$  and higher thrust production.
- Increase in mean free path due to rarefaction may affect power deposited to neutrals.
- With increasing  $[e]$ , increase in production of electronically excited states.

- 10 sccm Ar, 30 Torr at inlet, 10 Torr at exit.

# POWER DEPOSITION: FLOW VELOCITY



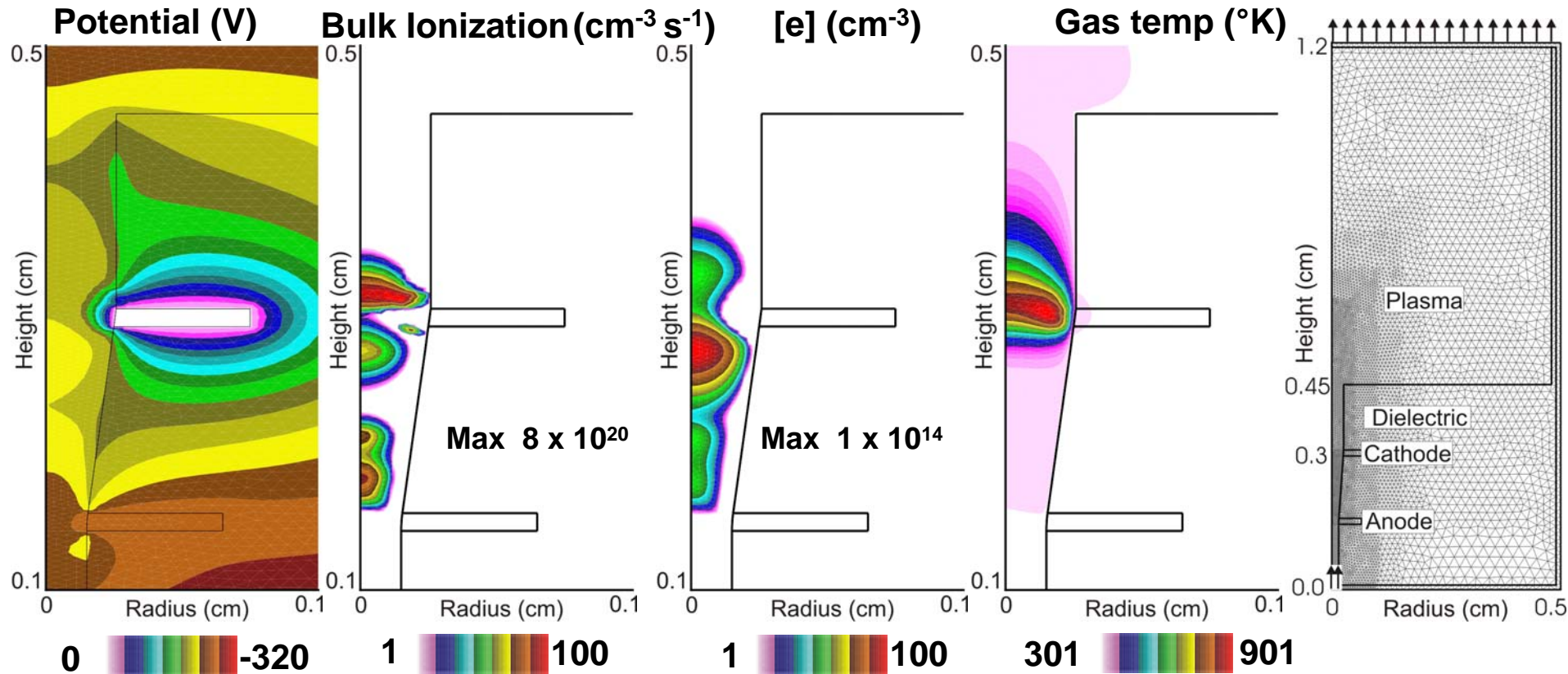
$V_y$  compared in the above plane.

- 10 sccm Ar, 30 Torr at inlet, 10 Torr at exit.
- Power turned on at 0.5 ms.

5 MAX  
Axial velocity (m/s)



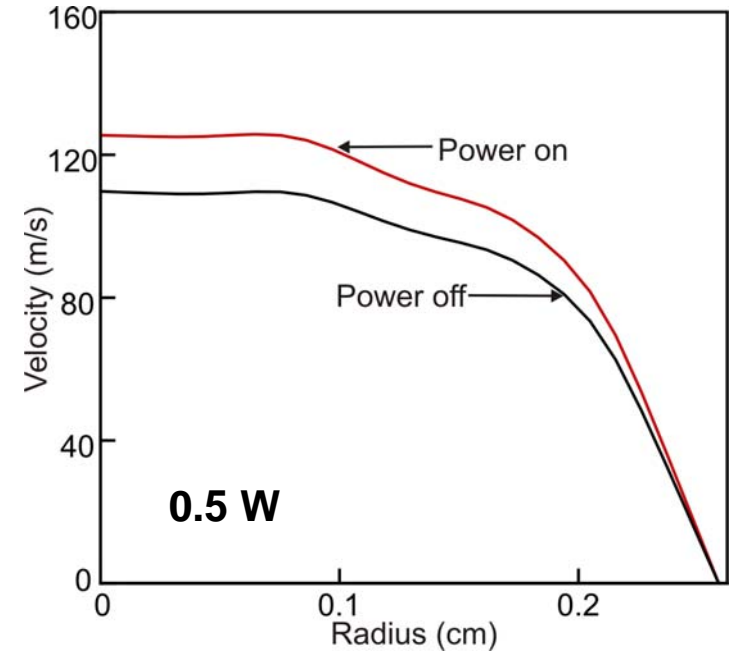
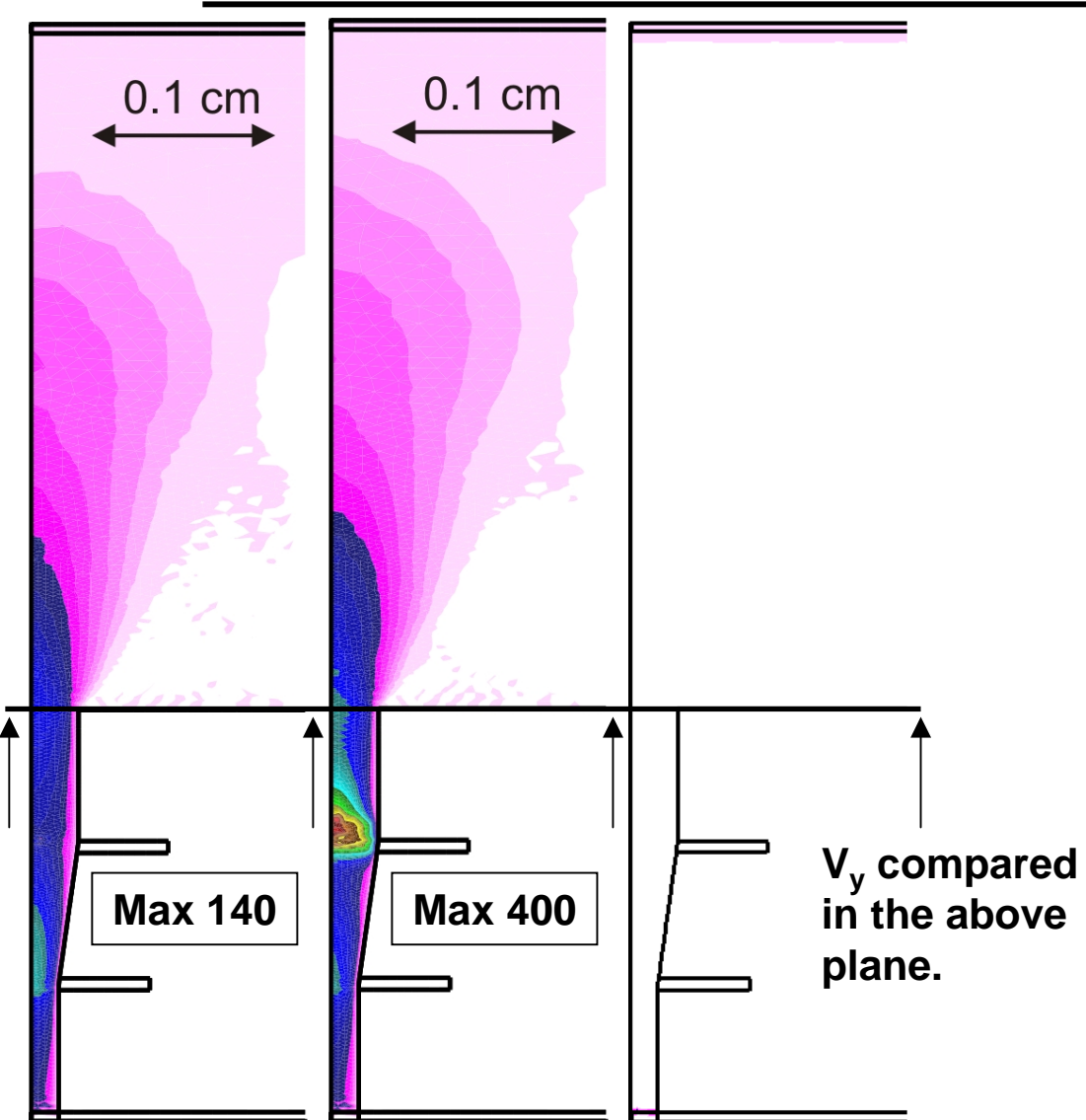
# BASE CASE RESULTS: GEOMETRY B



- Electrons are confined, discharge operates in an unsteady regime.
- Ionization pulses travel towards anode.
- Power densities are greater than that of Geometry A.

- 10 sccm Ar, 30 – 10 Torr
- 0.5 W, turned on at 0.5 ms

# VELOCITY INCREASE: GEOMETRY B



- Increase in velocity is due to expansion of hot gas.
- Axial-velocity increase not substantial at exit.
  - 10 sccm Ar, 30 – 10 Torr
  - 0.5 W, turned on at 0.5 ms

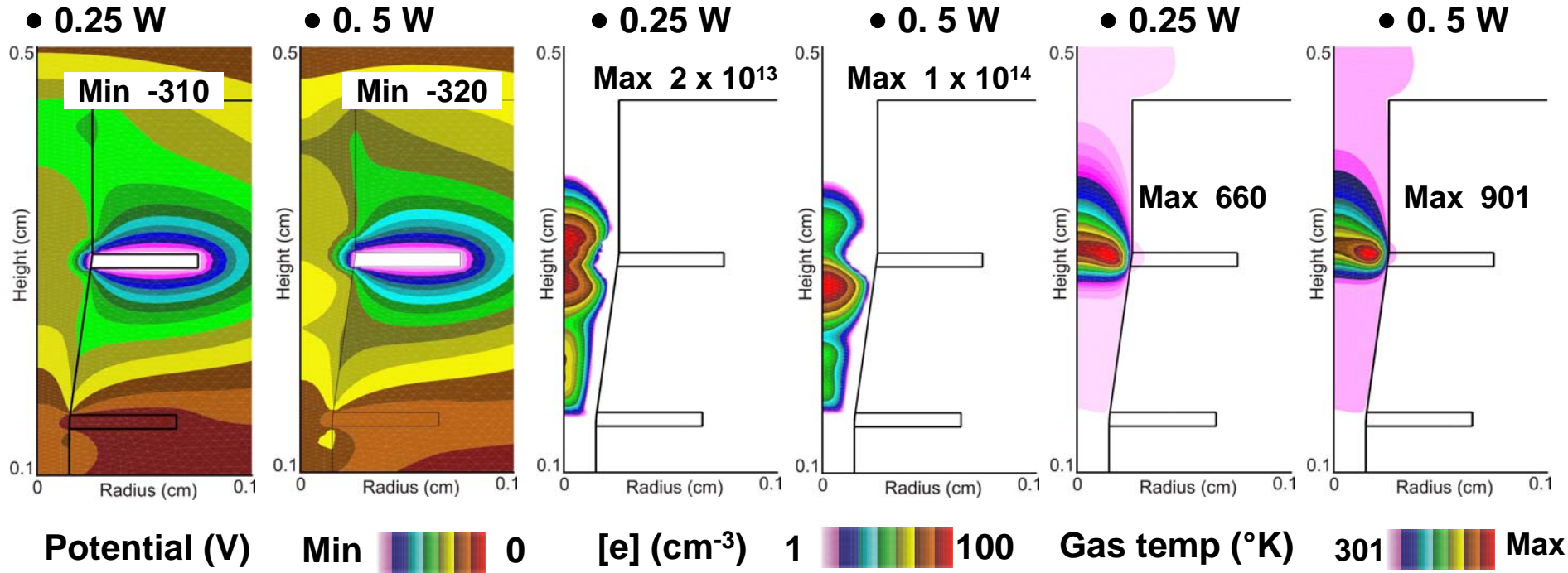
5 MAX Axial velocity (m/s)

AVS2005\_RAA\_17

Animation  
0 – 0.65 ms

Iowa State University  
Optical and Discharge Physics

# POWER DEPOSITION: GEOMETRY B



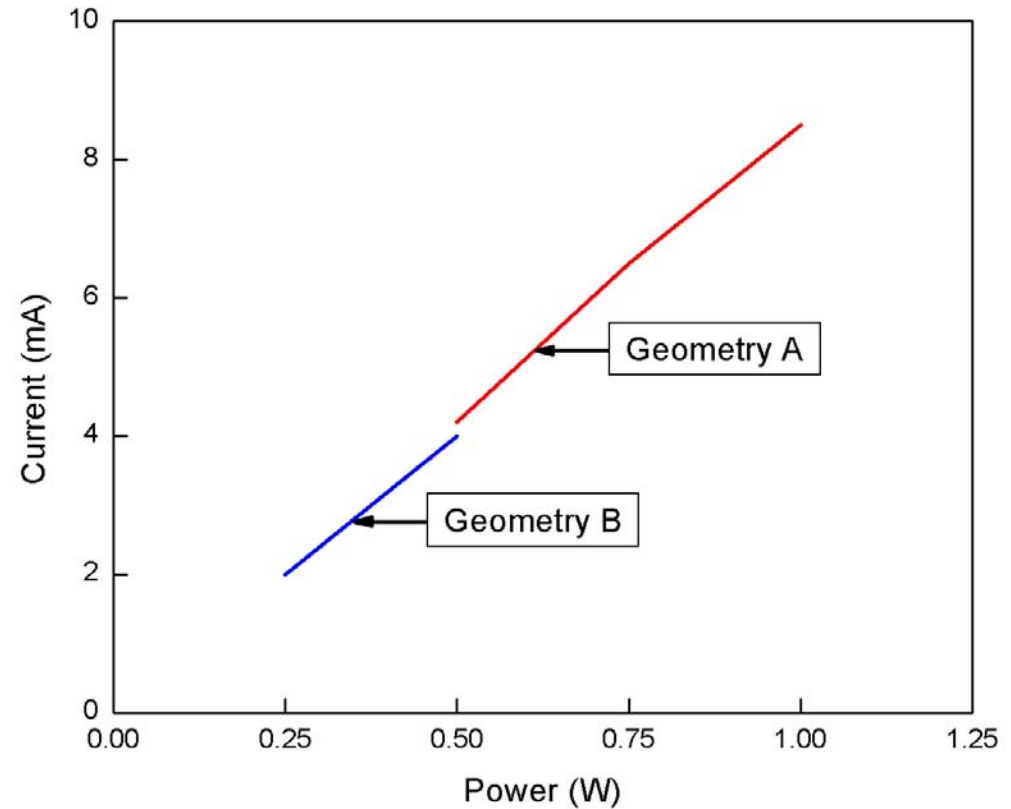
- Discharge operates in normal glow, current increases with power, whereas voltage marginally increases.
- [e] increases substantially with increase in power.
- With increasing [e], charge buildup on the dielectric can be high.

- 10 sccm Ar, 30 Torr at inlet, 10 Torr at exit.

# CURRENT VOLTAGE CHARACTERISTICS

---

- Operating voltage for geometry A remains almost a constant (260 V), whereas slight changes observed for geometry B.
- Discharge resistance  $R_D$  of 43 k $\Omega$ .



# INCREMENTAL THRUST

---

- Thrust calculated by:

$$F = \frac{dm}{dt} V_e + A_e (P_e - P_a)$$

- Increase in thrust is the rate of momentum transfer to the neutrals when the discharge is switched on.

$$\vec{\delta F} = \left( \frac{dm}{dt} \vec{V} \right)_{pulse} - \left( \frac{dm}{dt} \vec{V} \right)_{nopulse}$$

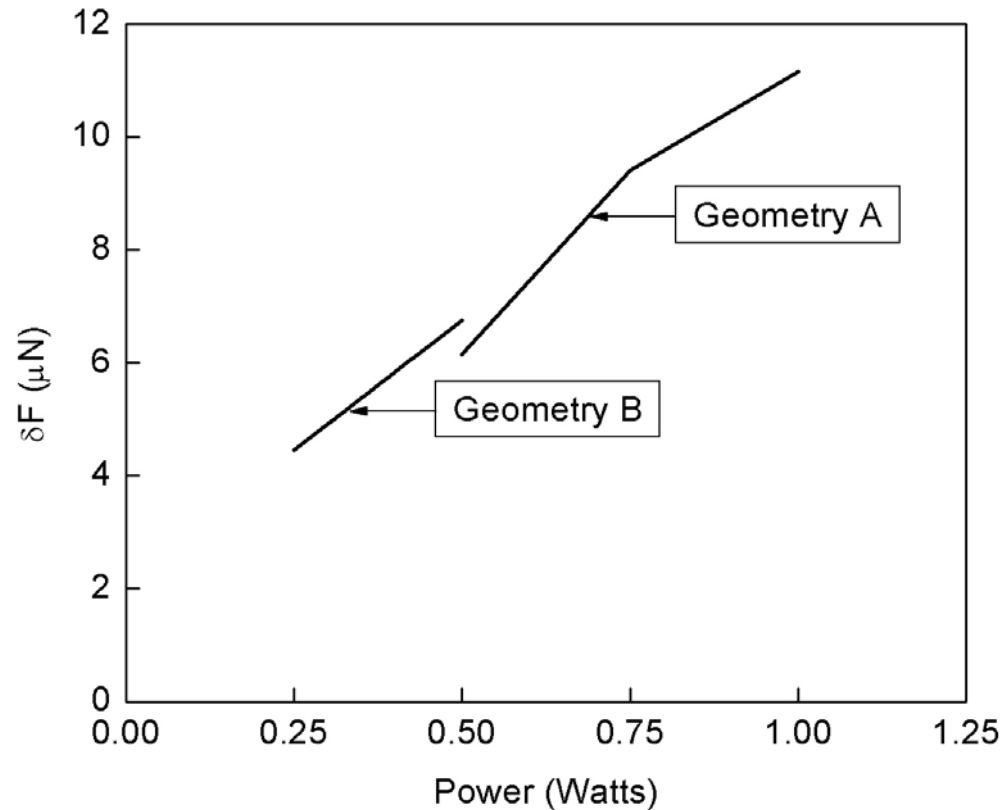
- Meaningful incremental thrust occurs when power deposited to plasma is greater than that contained in the flow.

$$\vec{j} \cdot \vec{E} \geq \frac{1}{2} \dot{\rho} v^2$$

# INCREMENTAL THRUST: EFFECT OF POWER

---

- Thrust increases with power deposited.
- Zero-power thrust:
  - Geometry A:  $8\mu\text{N}$
  - Geometry B:  $12\mu\text{N}$
- Geometry has marginal effect on incremental thrust.



- 10 sccm Ar, 30 Torr upstream, 10 Torr downstream.
- Power turned on at 0.5 ms

# CONCLUDING REMARKS

---

- **An axially symmetric microdischarge was computationally investigated with potential application to microthrusters.**
- **Studies were conducted to investigate the effect of parameters such as power deposition, and the geometry of the reactor.**
- **The geometry affected the plasma characteristics significantly, whereas there was no significant difference to incremental thrust.**
- **At higher power, higher gas temperatures lead to higher thrust.**
- **Rarefaction at high temperatures decreases mean free path and could limit thrust produced.**